SLAC-PUB-16239
March 2015

Flexible pulse delay control up to picosecond for high-intensity twin electron bunches*

Zhen Zhang[1,2], Yuantao Ding[1], Paul Emma[1], Agostino Marinelli[1], Zhirong Huang[1], Chuanxiang Tang[2]
[1] SLAC National Accelerator Laboratory, Menlo Park, CA 94025, USA
[2] Department of Engineering Physics, Tsinghua University, Beijing 100084, China

Abstract

Two closely spaced electron bunches have attracted strong interest due to their applications in two color x-ray free-electron lasers as well as witness bunch acceleration in plasmas and dielectric structures. In this paper, we propose a new scheme of delay system to vary the time delay up to several picoseconds while not affecting the bunch compression. Numerical simulations are performed to demonstrate the feasibility of this method.

Submitted to the Phys. Rev. ST Accel. Beams.

*Work supported by Department of Energy contract DE–AC02–76SF00515.

Flexible pulse delay control up to picosecond for high-intensity twin electron bunches

Zhen Zhang,[1,2] Yuantao Ding,[1] Paul Emma,[1]
Zhirong Huang,[1] Agostino Marinelli,[1] and Chuanxiang Tang[2]

[1]*SLAC National Accelerator Laboratory, Menlo Park, CA 94025, USA*
[2]*Department of Engineering Physics, Tsinghua University, Beijing 100084, China*

(Dated: March 18, 2015)

Two closely spaced electron bunches have attracted strong interest due to their applications in two color x-ray free-electron lasers as well as witness bunch acceleration in plasmas and dielectric structures. In this paper, we propose a new scheme of delay system to vary the time delay up to several picoseconds while not affecting the bunch compression. Numerical simulations are performed to demonstrate the feasibility of this method.

I. INTRODUCTION

The generation of two closely spaced electron bunches ("twin bunches") has been the subject of intense investigation in the recent past due to their application to diverse fields such as free-electron lasers (FELs) [1–3] and beam-driven plasma wakefield acceleration (PWFA) [4–6]. In an x-ray free-electron laser, twin bunches are used to generate two-color x-ray pulses [7] with large output power for time-resolved x-ray pump/x-ray probe experiments. They can also find applications in staged seeded FELs to reduce the spectral noise and the temporal jitter [8]. Furthermore the application of this concept to witness-bunch plasma-wakefield acceleration [9, 10], allows for greater flexibility in controlling the charge distribution, peak current and time delay, which can improve the performance of the PWFA.

The longitudinal dynamics of the twin bunches has been discussed in Ref. [11] including wakefield effects. Based on the analysis, the control of twin bunches is coupled with the compression of each individual bunch. So the final longitudinal separation, also called time delay, of the twin bunches is limited to roughly $\lesssim$ 300 fs under the requirement for high beam peak current. In this case, to further increase the time delay, a dedicated delay system could be considered. While electron dynamics typically happens on the scale of a few to tens of femtosecond, reaching picosecond delays is crucial for the time resolved investigation of nuclear motion in x-ray excited samples.

In this paper, we propose a new scheme of delay system to control the delay of twin electron bunches in picosecond range. We apply this system to the Linac Coherent Light Source (LCLS) [12]. Numerical simulations are performed to show that the delay system can vary the pulse delay up to several picoseconds while not affecting the compression of each individual bunch.

The paper is organized as follows. We begin in Sec. II with basic considerations and a detailed description of the new delay system. In Sec. III, we give some analysis of the delay system. In Sec. IV we discuss the application of this system to the LCLS and present the results of start-to-end numerical simulations. Finally, we give concluding remarks in Sec. V.

II. ELECTRON DELAY SYSTEM

In order to further increase the time delay while not sacrificing the intensity of single bunch, a dedicated delay system could be considered to be added into the two-stage-

compression beamline. The delay system need to have little effect on the compression of each bunch.

A magnetic chicane is usually used to delay the electrons. Consider the scenario shown in Fig. 1 (*a*). Two electron bunches with energy separation travel through a magnetic chicane. The extra time delay ΔT induced by the chicane is related to its R_{56} and the relative energy separation δ of the two bunches by

$$\Delta T = \frac{R_{56}\delta}{c} , \tag{1}$$

where c is the speed of light and we have assumed that each individual bunch itself is unchirped so that the compression due to the magnetic chicane is negligible. The achievable delay with this method is limited by the finite energy separation δ, which is typically constrained to a few percent by chromatic effects in the beam transport. For example, for two electron bunches with relative energy separation 1 %, if we want to increase their time delay by 1 ps, the $|R_{56}|$ of the chicane need to be 30 mm.

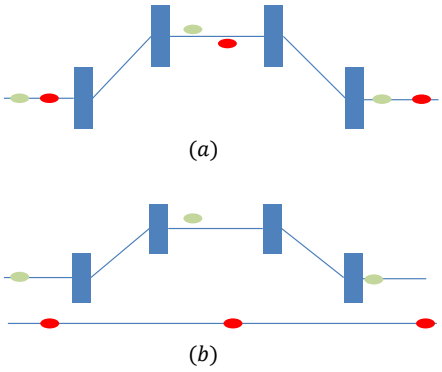

FIG. 1. A schematic layout of two different delaying methods: (*a*) the two bunches both go through the chicane and (*b*) only one of the two bunches goes through the chicane. The two bunches are assumed to have an initial time delay before the chicane.

Alternatively, if we only allow one of the two bunches go through the chicane, as shown in Fig. 1 (*b*), the extra time delay induced by the chicane will be

$$\Delta T = \frac{R_{56}}{2c} , \tag{2}$$

which is independent of energy separation. In this case, to increase the time delay by 1 ps, the required $|R_{56}|$ is only ∼0.6 mm and much smaller compared to the first method.

To only let one bunch go through the chicane, one possible way is to split the two electron bunches transversely. This can be achieved if the delay system is located in a dispersive section. In a high-energy linac, for example the LCLS, large dispersion usually appears in the middle of the large magnetic chicanes used for bunch compression. It follows that a small delay chicane added in the middle of the compression chicane can be used to increase the delay between the two bunches, as shown in Fig. 2.

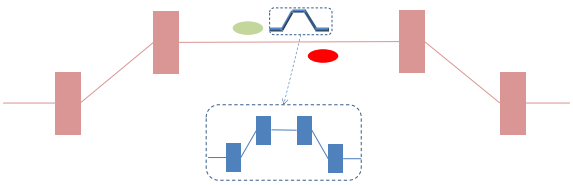

FIG. 2. A schematic layout of electron delay system (not to scale). The small chicane in the blue dashed square is inserted into the large chicane. The inserted chicane here is used to delay the low-energy bunch.

We can refer the small chicane in blue dashed square as "delay chicane". In the regular large chicane, the low (high)-energy bunch goes through the outer (inner) trajectory. The delay chicane can be used to delay either the low or high energy bunch. In Fig. 2 the chicane is illustrated to delay the low-energy bunch. If the extra introduced delay is of several picoseconds, the required $|R_{56}|$ of the delay chicane (∼ 1 mm) is much smaller

than the typical $|R_{56}|$ of a regular compression chicane ($\sim 30\,\mathrm{mm}$). Thus the delay chicane will have little effect on the compression of individual bunch. This also indicates that we can fully control the time delay through the delay chicane without changing other parameters in the beamline.

Since the transverse distance between the two bunches at the middle of the compression chicane is typically on the order of several millimeters, special care needs to be put in the design of the delay chicane. The four dipoles of the delay chicane will adopt septum magnets, which are normally used in the storage rings to kick beams for injection and extraction [13, 14]. Figure 3 shows the transverse cut of a septum magnet. The beam is stretched along x direction by the dispersion. There are two regions in the magnet: one is the vertical field region and the other is the field free region. The bunch in the vertical field region will be deflected and then pass through the delay chicane. For the design of the septum magnet, two parameters are very important: the beam-to-beam separation d_b and the barrier between field and field-free regions d_f. In a real design, the two parameters will be restricted by practical considerations such as shielding magnetic field to zero for generating the sharp field edge.

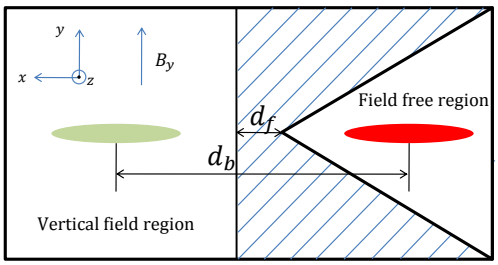

FIG. 3. Transverse cut of septum magnet (not to scale). The shaded area is the material to shield the magnetic fields. The red ellipses are the electron beam. This septum as shown here is used to delay the low-energy bunch (left bunch).

Note that the septum magnet in Fig. 3 is used to delay the low-energy bunch (or the bunch in the outer trajectory). To delay the high-energy bunch, the two regions in the magnet have to be changed and the vertical field needs to be reversed.

III. ANALYSIS OF ELECTRON DELAY SYSTEM

We now consider the dynamics of the electron delay system in Fig. 2 in the $x-z$ plane and hereafter neglect the uncoupled motion in vertical plane. Let the coordinate vector be $(x, x', z, \delta)^T$. We use rectangular bends for the delay chicane and its transfer matrix (R_d) can be written as

$$R_d = \begin{bmatrix} 1 & L_d & 0 & 0 \\ 0 & 1 & 0 & 0 \\ 0 & 0 & 1 & R_{56}^d \\ 0 & 0 & 0 & 1 \end{bmatrix} , \tag{3}$$

with L_d the total length and R_{56}^d the momentum compaction. Then the transfer matrix across the entire system is

$$R = R_2 R_d R_1 , \tag{4}$$

where R_1 and R_2 are the transfer matrices of the sections before and after the delay chicane. If we refer η as the dispersion in the middle of the large chicane and R_{56} as its momentum compaction, R_1 and R_2 can be written as

$$R_1 = \begin{bmatrix} 1 & L_1 & 0 & \eta \\ 0 & 1 & 0 & 0 \\ 0 & \eta & 1 & R_{56}/2 \\ 0 & 0 & 0 & 1 \end{bmatrix} ,$$

$$R_2 = \begin{bmatrix} 1 & L_2 & 0 & -\eta \\ 0 & 1 & 0 & 0 \\ 0 & -\eta & 1 & R_{56}/2 \\ 0 & 0 & 0 & 1 \end{bmatrix} , \tag{5}$$

with L_1 and L_2 the length of each section. Then the matrix of the full system is

$$R = \begin{bmatrix} 1 & L_1 + L_2 + L_d & 0 & 0 \\ 0 & 1 & 0 & 0 \\ 0 & 0 & 1 & R_{56} + R_{56}^d \\ 0 & 0 & 0 & 1 \end{bmatrix} . \tag{6}$$

Comparing this matrix with the one without a delay chicane, we can find that only the momentum compaction is increased by R_{56}^d. The delay chicane does not introduce other elements in the full transfer matrix, such as dispersion. Providing different R_{56} for the two bunches gives a new method to control the delay of two bunches.

The application of the septum magnets in the delay chicane puts extra requirements for the electron beam, since d_b and d_f in Fig. 3 cannot be too small. Assuming the beam transverse size along x dimension is dominated by the dispersion, then the transverse separation of the two bunches is

$$d_b = \eta\delta \ , \tag{7}$$

with δ the relative energy separation. For a fixed chicane, the minimum value of d_b will lead to the minimum available energy separation of the two bunches. The energy separation is induced by the off-crest acceleration as the two bunches are separated by T in the upstream linac, which can be written as

$$\delta = hT \ , \tag{8}$$

where h is the final energy chirp of the two bunches before compression and T is within the same RF bucket. This final energy chirp includes the energy chirp induced by radio-frequency (RF) curvature and wakefields, and also the initial chirp. For a fixed chicane system, we can estimate the final energy chirp by the R_{56} needed to transition into over compression [11],

$$h \approx \frac{1}{-R_{56}} \ . \tag{9}$$

A more accurate value of h should be a little larger, but this is still a good approximation. Then the transverse separation of Eq. 7 will become

$$d_b \approx \frac{\eta}{-R_{56}} T \ , \tag{10}$$

which is determined by the chicane system and initial longitudinal separation. The value of Eq. (10) needs to be larger than the minimum available value in the septum magnet.

In addition, the bunch length of individual bunch (L_b) is also limited, since the edge-to-edge distance of the two bunches needs to be larger than the barrier d_f to avoid beam loss. This condition can be written as

$$h\eta(T - L_b) > d_f \ . \tag{11}$$

Using Eqs.(7) and (8), we will have

$$\frac{L_b}{T} < 1 - \frac{d_f}{d_b} \ . \tag{12}$$

The ratio L_b/T is defined as duty factor in Ref. [11] to represent the structure of twin bunches.

IV. APPLICATION TO THE LCLS

In this section we apply the above electron delay system to the LCLS to control high-intensity twin bunches with tunable time delay up to several picoseconds. We assume typical beam parameters of a twin-bunch/two-color FEL so that the final peak current of each bunch is set to be $\sim 4\,\mathrm{kA}$. A schematic layout of the beamline with two-stage compression is shown in Fig. 4. The delay chicane is inserted in the middle of the second chicane (BC2). The incoming twin bunches before L1 are generated by the upstream injector with a variable delay on the order of a few picoseconds. The beam parameters after the injector are given in Table I. The total charge is 150 pC with 75 pC for each bunch and the initial time delay is 8 ps. The longitudinal phase space of the twin bunches before L1 is given in Fig. 5 with current profile. Here we assume a Gaussian distribution in time for each individual bunch and the beam centroid is accelerated on crest.

The designed delay chicane for the LCLS is shown in Fig. 6 with 2-m total length. The length of bend septum magnet is 20 cm. The drift length between the first and second, and

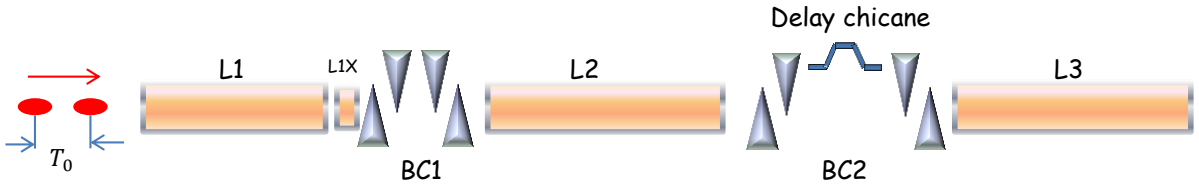

FIG. 4. A schematic layout of the LCLS beamline to generate the twin bunches (not to scale). The red ellipses are the electron beam after the injector. The delay chicane is inserted in BC2.

TABLE I. Beam parameters of the twin bunches after the injector.

Parameter	Value	Units
Total charge Q	150	pC
Beam energy E_0	135	MeV
Peak current I_p	32	A
Time delay T_0 [a]	8	ps
Bunch length σ_z [b]	0.9	ps
Slice energy spread σ_E	20	keV
Norm. emittance $\epsilon_{x(y)}$	0.4	mm-mrad

[a] T_0 is the time delay of the two bunches before BC1 compression.

[b] σ_z is the rms bunch length of individual bunch.

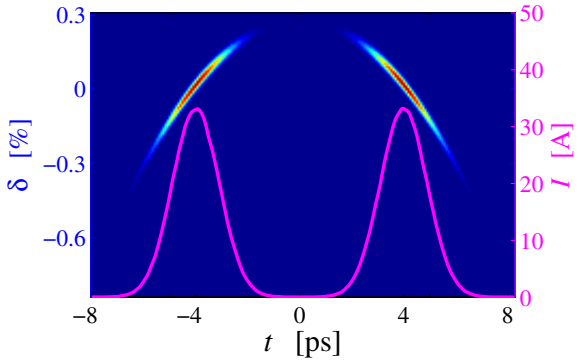

FIG. 5. Longitudinal phase space of the initial two bunches before L1 with current profile. The head bunch lies left.

also the third and fourth bend septum can be optimized to cover the required R_{56} range with reasonable magnetic field. In our case, the drift length is 50 cm and the required magnetic field is 0.7 T to achieve -1-mm R_{56}.

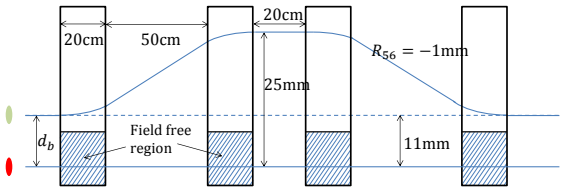

FIG. 6. A schematic layout of the delay chicane for the LCLS (not to scale). The largest transverse separation of the two orbits is 25 mm at $R_{56} = -1$ mm.

According to Eq. (10), large initial longitudinal separation in L2 between the twin bunches serves to increase the transverse distance before the delay chicane. However, in the case of large longitudinal separation, the energy chirp difference due to the RF curvature becomes non-negligible, which will generate different compression effects for the two bunches. In this case, we can set the first-stage chicane (BC1) at over compression to leave an opposite energy chirp on the beam compared with the one induced by L2. The energy chirp difference over the twin bunches after over compression can compensate the energy chirp difference from L2 to make the two bunches have similar behavior in compression. This can be understood by the following simulation results.

We use Elegant [15] to simulate the acceleration and compression of the two bunches

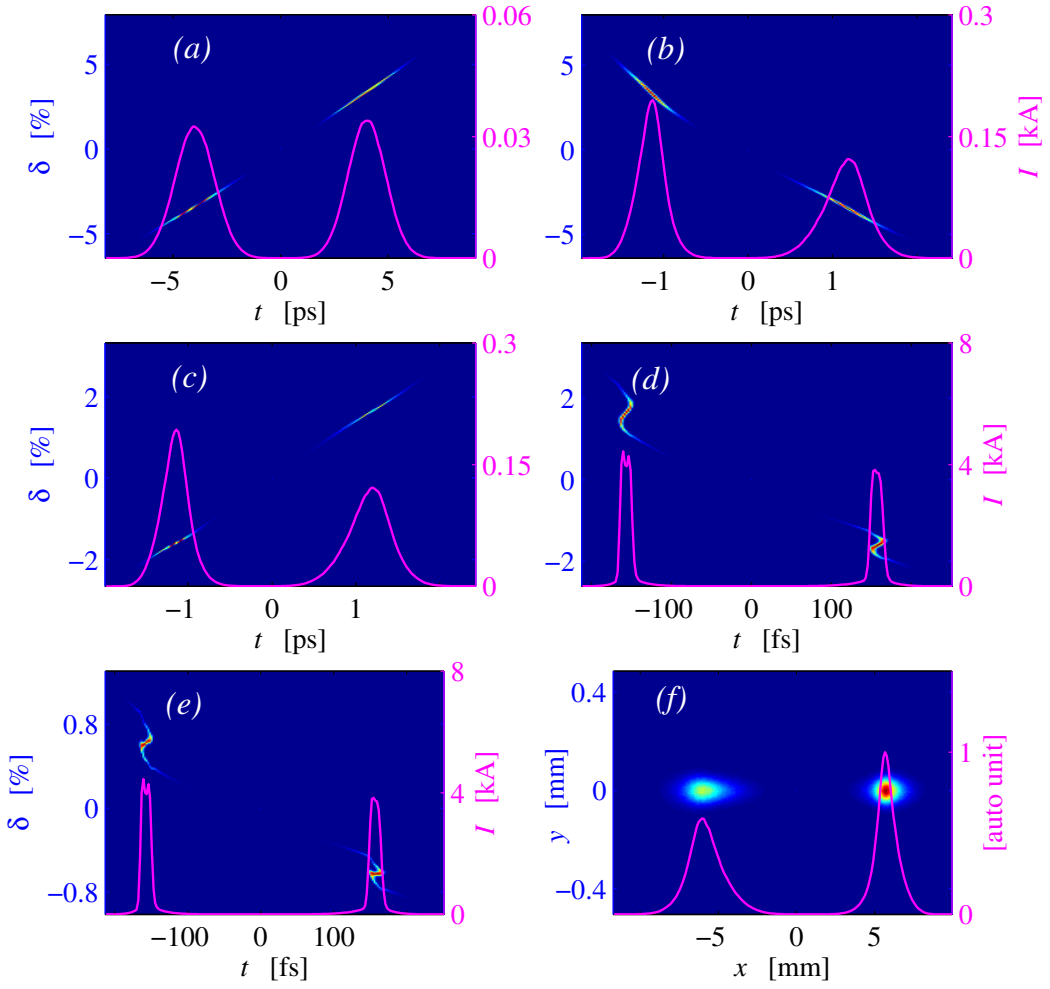

FIG. 7. Longitudinal phase space evolution with current profile without the delay chicane : (*a*) BC1 entrance; (*b*) BC1 end; (*c*) BC2 entrance; (*d*) BC2 end; (*e*) L3 end. (*f*) is the transverse distribution of the two bunches with intensity profile in the middle of BC2. The L1 phase is $-35.5\,^\circ$ and the L2 phase is $-41.7\,^\circ$.

with collective effects. In the simulation, for simplicity, we vary the off-crest acceleration phases of L1 and L2 to optimize the compression of BC1 and BC2 while keeping other parameters fixed. The beamline parameters are shown in Table II. Note that when the phases of L1 and L2 are changed, the corresponding RF amplitude will be adjusted to keep the same beam energy at BC1 and BC2. The R_{56} of BC2 is -24.7 mm and the corresponding dispersion is 36.3 cm.

Figure 7 gives the longitudinal phase space evolution and the transverse distribution in the middle of BC2. The R_{56} of the delay chicane is 0 in the simulation. The L1 phase is set at $-35.5\,^\circ$ to make BC1 at over compression, which can be seen from Fig. 7 (*b*). As discussed in Ref. [11], BC2 is set at over compression to let the high-energy bunch come first while the compression of each individual bunch is under compression to obtain flat energy chirp under the effect of wakefields. At the end of L3, as shown in Fig. 7 (*e*), the peak current of the two bunches are both ∼4 kA

TABLE II. Beamline parameters of the LCLS to generate twin bunches.

Parameter	Value	Units
BC1 energy E_1	220	MeV
BC2 energy E_2	5	GeV
BC2 peak dispersion η	36.3	cm
Final energy E_3	13.5	GeV
R_{56} of BC1	-45.5	mm
R_{56} of BC2	-24.7	mm
L1X amplitude E_X	22	MeV
L1X phase ϕ_X	-160	deg
L1 phase ϕ_1	-20∼-40	deg
L2 phase ϕ_2	-30∼-45	deg

with time delay 310 fs and energy separation 1.2 %. Due to the large energy separation before BC2 (∼3% in Fig. 7 (*d*)), the beam-to-beam horizontal separation before the delay chicane is about 11.5 mm and the edge-to-edge separation is > 5 mm If we consider $\pm 3\sigma$ range of the transverse distribution, as shown in Fig. 7 (*f*). These two numbers are reasonable for the application of septum magnets.

The wakefields of the septum magnet, including the step-out and resistive wall wakes, are both considered as the wake-induced energy loss may deteriorate the beam emittance after compression [16]. However, due to the low beam peak current (∼250 A) and high beam energy in the septum magnet, the wake-induced emittance increase is negligible (~ 0.5 %) in our case.

We can choose either the high or low energy bunch to pass through the delay chicane to control the time delay. Here we take the low-energy bunch as an example. For the beam in Fig. 7, we vary the $|R^d_{56}|$ of the delay chicane from 0 to 1 mm. The simulation results are shown in Fig. 8. As increasing $|R^d_{56}|$, the longitudinal phase space of each individual bunch keeps almost the same with the one in Fig. 7 (*e*) but the final time delay (T_f) of the two bunches is extended linearly up to $\sim$ 2 ps (see Fig. 8 (*a*)). The final energy separation is almost unchanged. The peak current of the delayed bunch in Fig. 8 (*b*) has a little growth due to the compression effect of the delay chicane. However, the peak current is still in reasonable range and the growth can be compensated by making a small change for the phases of L1 and L2.

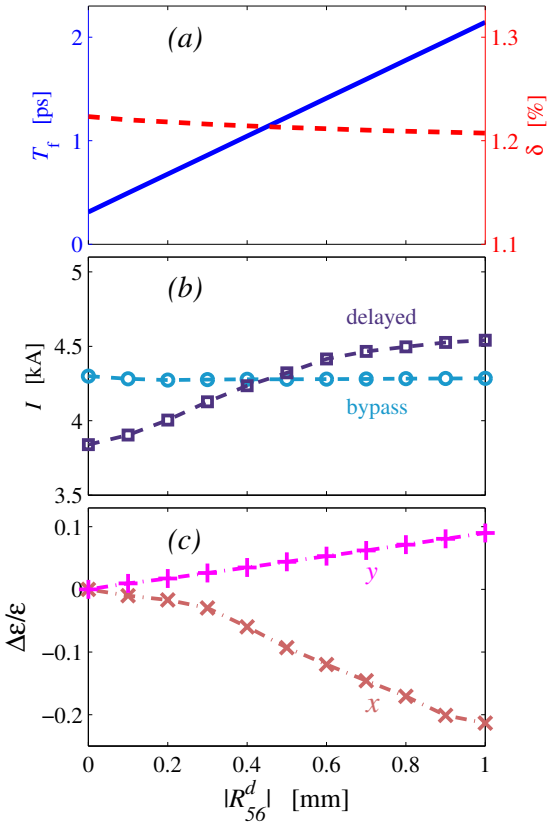

FIG. 8. Parameters of the twin bunches versus the R^d_{56} of the delay chicane. (*a*): final time delay (blue solid line) and energy separation (red dashed line); (*b*): peak current of the delayed bunch (square) and the bypass bunch(circle); (*c*): the projected emittance changes of the twin bunches in x (cross) and y (plus) planes.

The delay chicane also has effects on the emittance of the twin bunches. When the R^d_{56} of the delay chicane is 0, the final projected emittane of the two bunches at the end of L3 is ∼1 mm-mrad in horizontal plane and ∼0.6 mm in vertical plane. The increase of the horizontal projected emittance is mainly resulted from coherent synchronous radiation

(CSR) and chromatic effect as the energy spread of the two bunches is large compared with the designed beamline optics. Increasing the R_{56}^d of the delay chicane, the horizontal projected emittance decreases. This is because the additional longitudinal delay from the delay chicane avoids generating ultra-high peak current when the two bunches overlap during compression, and hence reduces the CSR effect. The increase of the vertical projected emittance of the two bunches comes from the chromatic effect and beam optics setup. The vertical projected emittance of each individual bunch is preserved well during the whole beamline. In the simulation for this study, we used the LCLS optics designed for single bunch. To optimize the emittance of the two bunches, the optics needs to be redesigned for the two bunches with large energy separation.

V. CONCLUSION

In this paper, we proposed a new method to generate high-intensity twin electron bunches with ps-level delay. Our method relies on the use of a delay chicane in a high-dispersion region that selectively delays one of the two bunches by means of four septum magnets. We apply this method to the LCLS and discuss the optimization of the beam parameters for two-color x-ray FEL operation. The results of numerical simulations demonstrate that with the proposed delay system, we can change the time delay between twin bunches up to several picoseconds with stable peak current and energy separation.

VI. ACKNOWLEDGMENTS

We would like to thank Karl Bane and Jerome Hastings for helpful discussion. This work was supported under US Department of Energy contract DE-AC02-76SF00515.

[1] J. Madey, J. Appl. Phys. 42, 1906 (1971).
[2] A. Kondratenko and E. Saldin, Part. Accel. 10, 207 (1980).
[3] R. Bonifacio, C. Pellegrini, and L. Narducci, Opt. Commu. 50, 373 (1984).
[4] P. Chen, J. M. Dawson, Robert W. Huff, and T. Katsouleas, Phys. Rev. Lett. 55, 1537 (1985).
[5] J. Rosenzweig, Phys. Rev. Lett. 58, 555 (1987).
[6] C. Joshi, et al., Nature 377, 606 (1995).
[7] A. Marinelli et al., Nat. Commun. 6, 6369 (2015).
[8] L.H. Yu, in *"Mini-Workshop on Present and Future FEL Schemes"*, 2008, Shanghai.
[9] M. J. Hogan et al., New Journal of Physics 12 (2010) 055030.
[10] M. Litos et al., Nature 515, 92-95 (2014).
[11] Z. Zhang, Y. Ding, A. Marinelli, and Z. Huang, Phys. Rev. ST Accel. Beams 18, 030702 (2015).
[12] P. Emma et al., Nat. Photonics 4, 641 (2010).
[13] Glea R. Lanibertsoa, "LAMBERTSON." U.S. Patent No. 3,128,405. 7 Apr. 1964.
[14] A. Hilaire, V. Mertens, E. Weisse, No. LHC-Project-Report-208. 1998.
[15] M. Borland, ELEGANT, Advanced Photon Source LS-287, 2000.
[16] K. Bane and T. Raubenheimer, in the proceedings of *the 25th North American Particle Conference*, NaPAC'13, Pasadena, California, 2013.